The Bioscan AN INTERNATIONAL QUARTERLY JOURNAL OF LIFE SCIENCES 21(2): S.I(2),1226-1255, 2026 www.thebioscan.com

Sustainable Microbial Synthesis of Ti–ZnO Nanocomposites: A Multifunctional Platform for Biomedical Applications

Prajwal D. Nikam[a, b], Sanghamitra M. Kamble[a, b], Prachi P. Chavan[a, b], Bhakti R. Kalaskar[a, b], Akansha P. Badekar[a, c], Avinash A. Survase[a, b, *]

[a] Department of Microbiology, Yashavantrao Chavan Institute of Science, Satara-415001, Maharashtra, India

[b] Karmaveer Bhaurao Patil University, Satara-415001, Maharashtra, India

[c] Department of Microbiology, Lal Bahadur Shastri College, Satara, 415002, Maharashtra, India

Corresponding author* E-mail id: surwasedada09@gmail.com

DOI: https://doi.org/10.63001/tbs.2026.v21.i02.S.I(2).pp1226-1255

Keywords:

Aspergillus niger,
Ti-ZnO nanocomposite,
Biophysical analysis,
Biomedical applications.

Received on: 28-04-2026
Accepted on: 16-05-2026
Published on: 26-05-2026

Abstract

The present study reports the eco-friendly microbial synthesis of titanium–zinc oxide (Ti–ZnO) nanocomposites using a sustainable and cost-effective biological approach. The synthesized nanocomposite was comprehensively characterized using UV–Visible spectroscopy, X-ray diffraction (XRD), scanning electron microscopy (SEM), energy-dispersive X-ray spectroscopy (EDX), and Fourier transform infrared (FT-IR) spectroscopy. XRD analysis confirmed the crystalline anatase phase of TiO_2, while FT-IR spectra indicated the formation of Zn–O–Ti bonds, suggesting successful integration of ZnO within the TiO_2 matrix. SEM images revealed well-distributed nanoparticles, and EDX analysis verified the elemental composition and uniform incorporation of ZnO into TiO_2. The formation of the Ti–ZnO heterostructure significantly enhanced charge separation efficiency and reduced electron–hole recombination. Furthermore, the nanocomposite demonstrated notable biological activities, including anticancer, antidiabetic, antioxidant, and antimicrobial effects. These findings highlight the promising potential of microbial synthesized Ti–ZnO nanocomposites for diverse biomedical and therapeutic applications.

1. Introduction

Nanotechnology is rapidly growing field past few decades, It playing a significant role in various sectors, including the environment, industry, agriculture, and medicine [1–3]. The integration of nanotechnology with biotechnology has given rise to the emerging field of nanomedicine, which has enabled novel approaches for disease treatment, targeted drug delivery, and advanced diagnostics

[4,5]. Despite these advancements, the use of microbially synthesized nanoparticles produced through eco-friendly or "green" methods remains limited in biomedical applications [6]. This work focuses on the microbial synthesis of nanomaterials as a sustainable alternative and discusses their current and potential uses in the healthcare sector [7]. Zinc oxide (ZnO) is a widely utilized catalyst with significant industrial relevance, particularly in the fields of textiles, cosmetics, and pharmaceuticals [8]. Its broad applicability is attributed to a unique combination of physicochemical characteristics, including a wide direct bandgap energy (~3.37 eV), high exciton binding energy (~60 meV), thermal and chemical robustness, biocompatibility, non-toxicity, and distinct optoelectronic and piezoelectric properties [9,10]. Traditional physical and chemical synthesis routes for ZnO nanoparticles (ZnO NCs) are commonly employed; however, they are often limited by high energy demands, low sustainability, and the use of hazardous chemicals, raising concerns regarding environmental and economic viability [11]. In response, biosynthetic methods have emerged as promising eco-friendly alternatives [12]. These approaches leverage biological entities such as plant extracts or microorganisms as reducing and stabilizing agents to facilitate nanoparticle formation under mild conditions [13]. A variety of plant species have been successfully employed in the green synthesis of ZnO NCs due to their phytochemical content, which serves as natural capping and reducing agents [14]. Beyond plant-mediated synthesis, microbial systems have also been explored for nanoparticle production [15]. Bacteria, fungi, and algae possess metabolic pathways capable of reducing metal ions to their nanoparticulate forms [16]. In particular, fungi have been extensively studied due to their high metal

tolerance, extracellular enzyme secretion, and ease of biomass handling [17]. Various fungal strains including species of Aspergillus, Fusarium, Candida, Saccharomyces, and Stereum have demonstrated efficacy in synthesizing ZnO nanoparticles, offering a scalable and sustainable platform for nanomaterial production [18, 19].

Titanium (Ti) is widely recognized for its superior biocompatibility, attributed to its excellent mechanical strength, high resistance to corrosion, and minimal cytotoxicity [20]. These characteristics make it particularly suitable for use in biomedical applications, such as orthopedic and dental implants [21]. In nanoparticulate form, titanium dioxide (TiO_2) has attracted significant attention across various fields, including energy generation, environmental remediation, and biomedical applications [22]. TiO_2 utility largely stems from its wide band gap of approximately 3.2 eV, enabling strong photocatalytic activity through the generation of electron–hole pairs upon light absorption [23]. Enhancing photocatalytic performance often involves strategies to prolong the lifetime of charge carriers, thereby minimizing their recombination [24]. Doping ZnO with other metals or oxides, such as titanium, has been shown to modulate the band structure, facilitate more efficient charge separation, and improve the generation of reactive oxygen species (ROS) [25]. Generated ROS play a crucial role in antimicrobial activity by inducing oxidative damage to microbial membranes, proteins, lipids, and nucleic acids, ultimately leading to cell death or growth inhibition [26]. Nanoparticles such as ZnO, TiO_2, Ag, and CuO have demonstrated potent antimicrobial properties through these oxidative stress mechanisms [27]. Such characteristics are particularly valuable in high-moisture environments like textiles worn close to the body, where microbial contamination can cause odor formation, material degradation, and reduced product quality [28]. The incorporation of antimicrobial coatings, including ZnO-based nanoparticles, offers an effective strategy to control microbial growth on textile surfaces [29]. Among fungi, *Aspergillus niger* is notable for its high enzymatic activity and ability to produce a variety of intracellular and extracellular enzymes, including proteases, amylases, cellulases, and lipases [30]. These enzymes contain functional groups such as amines and carboxyls that facilitate the biosynthesis and stabilization of nanoparticles [31].

In present study investigates the biosynthesis of titanium-doped zinc oxide (Ti/ZnO) nanoparticles using enzyme-rich extracts from *A. niger* as capping and stabilizing agents [32]. The synthesis follows a sol–gel approach involving hydrolysis, condensation, aging, and calcination steps [33]. During condensation, bioenzymatic components regulate particle growth, prevent agglomeration, and ensure uniform nanoparticle distribution [34]. The Ti/ZnO nanoparticles antimicrobial activity was evaluated against Gram-positive and Gram negative bacterium[35].

2.0 Material and Method

2.1 Chemicals and Media

All analytical grade reagents were employed throughout the study. Titanium chloride ($TiCl_3$), zinc sulfate ($ZnSO_4$), ethyl acetate ($C_4H_8O_2$), free radical scavenger 2,2-diphenyl-1-picrylhydrazyl (DPPH) were obtained from Sigma-Aldrich (USA). Microbial growth media, including Sabouraud's dextrose broth, Mueller–Hinton broth (MHB) and nutrient broth procured from Hi-Media, India Ltd.

2.2 Isolation and identification of *fungi*

Soil samples were collected from five different locations in Satara, Maharashtra, India. Each sample was serially diluted up to 10^{-5} and spread on Sabouraud's dextrose agar plates. After incubation at 37 °C for 72 hours, distinct fungal colonies were isolated. In total, twenty-five fungal strains were obtained and preserved at 4 °C for further nanocomposite (NCs) synthesis.

2.3 Synthesis of Ti-ZnO nanocomposite using fungi

The synthesis of titanium dioxide (TiO_2) nanoparticles (NPs) was carried out using a microbial reduction approach. A total of ten fungal isolates were screened for their potential to mediate Ti-ZnO NCs formation. Each fungal strain was cultured in a 250 mL Erlenmeyer flask containing 100 mL of Sabouraud's dextrose broth and incubated at 37 °C on a rotary shaker operating at 140 rpm for 72 hours to promote mycelial growth. The developed fungal biomass was separated using Whatman No. 1 filter paper (Whatman, UK) and washed twice with Milli-Q water to remove residual media components. Approximately 15 g of freshly harvested mycelia were then transfer into 100 ml and incubated again at 37°C for 62 hours under continuous shaking (140 rpm) to obtain the extracellular fungal filtrate. The resulting cell-free filtrate was then treated with titanium chloride ($TiCl_3$) and zinc sulfate ($ZnSO_4$) at a final concentration of 10^{-5} M and incubated at 37 °C with agitation (140 rpm) for 48 hours to facilitate the biosynthesis of fine, monodispersed Ti-ZnO NCs through biotransformation. Among the ten tested fungal strains, one isolate exhibited significant NCs synthesis efficiency, indicating its superior potential for Ti-ZnO NCs production [36].

2.4 Material and Characterization

For the confirmation and comprehensive characterization of Ti–ZnO nanocomposite (Ti–ZnO NCs), a series of advanced analytical techniques were employed. The optical properties were evaluated using UV–Visible spectroscopy, which revealed distinct absorption peaks at specific wavelengths, confirming the optical behaviour of the nanostructures. Functional groups associated with the nanoparticles were investigated through Fourier Transform Infrared Spectroscopy (FTIR), where characteristic vibrational bands provided evidence of surface functional moieties and possible capping agents. The crystalline phase and structural arrangement of the Ti–ZnO NCs were determined by X-ray Diffraction (XRD) analysis. The average crystallite size was further calculated using the Debye–Scherrer equation, confirming particles are in nanometer-scale dimensions. Surface morphology of particles were examined through Scanning Electron Microscopy (SEM). Additionally, the elemental composition and purity of the nanomaterials were verified using Energy Dispersive X-ray Spectroscopy (EDS), which confirmed the presence of titanium, zinc and oxygen as the principal constituents, with no significant impurities detected [37].

2.5 Antimicrobial assay:

The antimicrobial activity of Ti–ZnO NCs was assessed using the agar well diffusion method. For antibacterial evaluation, sterile Mueller–Hinton (MH) agar plates were prepared and spread with 0.1 mL of pathogenic bacterial suspension. Wells were aseptically created on the agar surface, and Ti–ZnO NCs dispersed in sterile distilled water for introduced into the wells. The plates were then incubated at 37 °C for 24 hours. Each experiment was conducted in triplicate to ensure reproducibility of antibacterial activity. Following incubation, the diameters of inhibition zones surrounding each well were measured to determine the antimicrobial efficacy of the nanoparticles. For comparative analysis, standard drug controls were included: streptomycin served as the reference compound in antibacterial assays [38].

2.6 Anticancer study:

The cytotoxic activity of the samples was evaluated using the MTT assay on MCF-7 cells. The cells were initially cultured in growth medium at a density of 1 × 10^4 cells/mL and incubated for 24 h at 37 °C in a humidified atmosphere containing 5% CO_2. Subsequently, 100 µL of the cell suspension (1 × 10^4 cells/well) was seeded into 96-well tissue culture plates and allowed to attach. Different concentrations of the test samples (20, 40, 60, 80, and 100 µg/mL) were then added to the wells. Control wells contained cells treated with 0.2% DMSO in PBS. All experiments were performed in triplicate to ensure accuracy. The plates were incubated again for 24 h at 37 °C with 5% CO_2 in a CO_2 incubator. After incubation, the culture medium was carefully removed and 20 µL of MTT solution (5 mg/mL in PBS) was added to each well. The plates were then incubated for 4 h at 37 °C, allowing viable cells to convert the yellow MTT reagent into dark purple formazan crystals. The formation of these crystals was confirmed under a microscope. Following incubation, the medium was completely discarded and 200 µL of DMSO was added to each well to dissolve the formazan crystals. The plates were kept for 10 minutes at 37 °C, protected from light using aluminum foil. Finally, the absorbance of each well was measured at 550 nm using a microplate reader. The results were used to determine cell viability and cytotoxic activity of the tested samples [39].

2.7 Antioxidant activity:

The antioxidant potential of the test compounds was evaluated by measuring their free radical scavenging activity using the DPPH assay. In this method, 1 mL of the test samples at different concentrations (20, 40, 60, 80, and 100 µg/mL) was taken in separate test tubes. To each tube, 1.5 mL of 0.1% methanolic DPPH solution was added and the mixtures were incubated in the dark for 30 minutes to allow the reaction to occur. Following incubation, the change in color from deep purple to yellow indicated the reduction of DPPH radicals by the antioxidant compounds. The absorbance of each sample was then measured at 510 nm using a colorimeter. The percentage of free radical scavenging activity was calculated using the appropriate equation [40].

$$\text{DPPH scavenging effect (\%)} = \frac{A_0 - A_1}{A_0} X\ 100 \quad \ldots\ldots\ldots\ldots\ldots\ldots(1)$$

2.8 Antidiabetic Assay:

The in vitro α-amylase inhibitory activity was evaluated using the method described by Sumner Bernfeld with slight modifications. In this assay, 100 µL of the test compound at different concentrations (20, 40, 60, 80, and 100 µg/mL) was mixed with 500 µL of 0.1 M phosphate buffer (pH 6.9) containing α-amylase enzyme (fungal diastase, 0.5%). The reaction mixture was incubated at 25 °C for 10 minutes. Subsequently, 500 µL of 1% starch solution prepared in 0.1 M phosphate buffer (pH 6.8) was added and the mixture was further incubated at 25 °C for another 10 minutes. For the control experiment, 500 µL of phosphate buffer was used instead of the enzyme solution. After incubation, 1000 µL of dinitrosalicylic acid (DNS) reagent was added to both the test and control mixtures to terminate the reaction. The tubes were then placed in a boiling water bath for 10 minutes, followed by cooling to room temperature. The absorbance of the resulting solution was measured at 540 nm using a spectrophotometer. The percentage inhibition of α-amylase activity was subsequently calculated using the appropriate formula [41].

$$Inhibition\ (\%) = \frac{Abs\ 540\ (Control) - Abs\ 540\ (Extract)}{Abs\ 540\ (Control)} X\ 100 \quad \ldots\ldots\ldots\ldots\ldots\ldots(2)$$

3.0 Results and discussion:

3.1 Microbial synthesis of Ti-ZnO NCs

The isolated *Aspergillus niger* fungal supernatant was challenged with precursor metal salts for nanocomposite synthesis. Titanium chloride ($TiCl_3$) and zinc sulfate ($ZnSO_4$) precursor's were added at final 10^{-5} M concentrations. The reaction mixture was incubated at 37°C with continuous shaking (140 rpm) for 48 hours. The brownish black color precipitate formation indicates biotransformation of Ti-ZnO nanocomposites.

3.2 Characterization of the Ti-ZnO NCs

3.2.1. UV–visible spectroscopy

The UV–Visible Spectroscopy absorption spectrum represents the optical properties of Ti–ZnO nanocomposites in **Fig. 1**. The graph shows a strong absorption peak at 272 nm, which indicates the characteristic electronic transition associated with the nanocomposite structure. The high absorbance in the UV region confirms the ability of Ti–ZnO nanocomposites to absorb ultraviolet light efficiently. Beyond 300 nm, the absorbance decreases gradually, showing a broad tail that extends into the visible region, which suggests the presence of surface defects or oxygen vacancies contributing to light absorption. Overall, the result demonstrates that Ti–ZnO nanocomposites possess a prominent UV absorption edge around 272 nm, making them suitable for applications in photocatalysis, UV shielding, and optoelectronic devices [42].

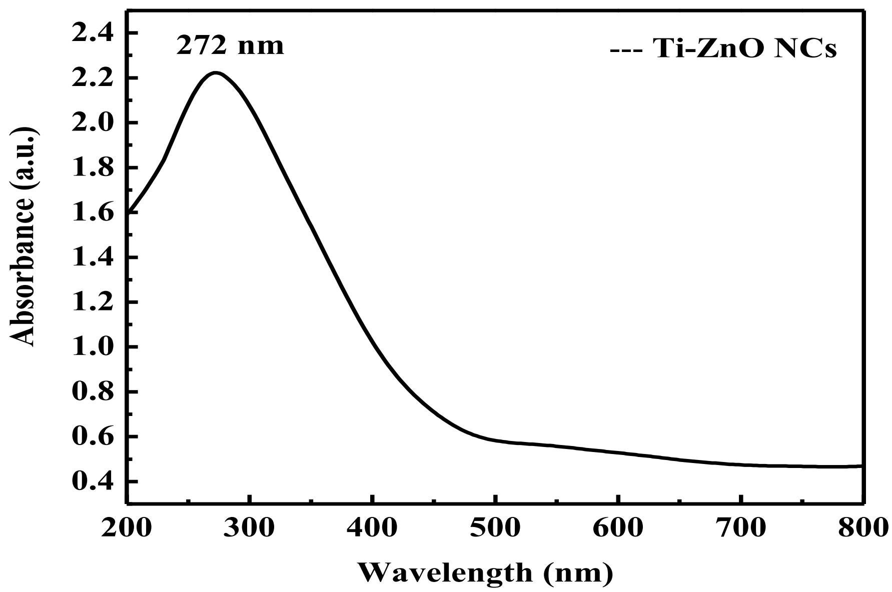

Fig. 1 UV-visible spectrum of Ti-ZnO NCs

3.2.2 Fourier Transform Infrared Spectroscopy (FTIR)

The FTIR spectrum of Ti-ZnO nanocomposites demonstrates distinct vibrational features that confirm the successful formation of the composite in **Fig 2**. A broad absorption band at 3430 cm^{-1} is assigned to O–H stretching, indicating surface hydroxyl groups and adsorbed moisture. Peaks at 2977 and 2920 cm^{-1} correspond to C–H stretching of aliphatic groups, most likely due to residual organics from the synthesis process. The absorption at 1628 cm^{-1} arises from H–O–H bending of adsorbed water, whereas the sharp band at 1397 cm^{-1} suggests contributions from C=O or O–H bending vibrations. Importantly, the strong features at 1093 and 1046 cm^{-1} can be associated with Ti–O–Ti and Ti–O–Zn bonds, providing evidence of titanium incorporation into the ZnO network. Finally, the band near 880 cm^{-1} is attributed to metaloxygen lattice vibrations, confirming the presence of Ti-ZnO linkages within the composite structure [43]. These observations collectively confirm the successful integration of titanium into ZnO nanoparticles, resulting in the formation of Ti–ZnO nanocomposites with distinct functional groups and bonding characteristics [44].

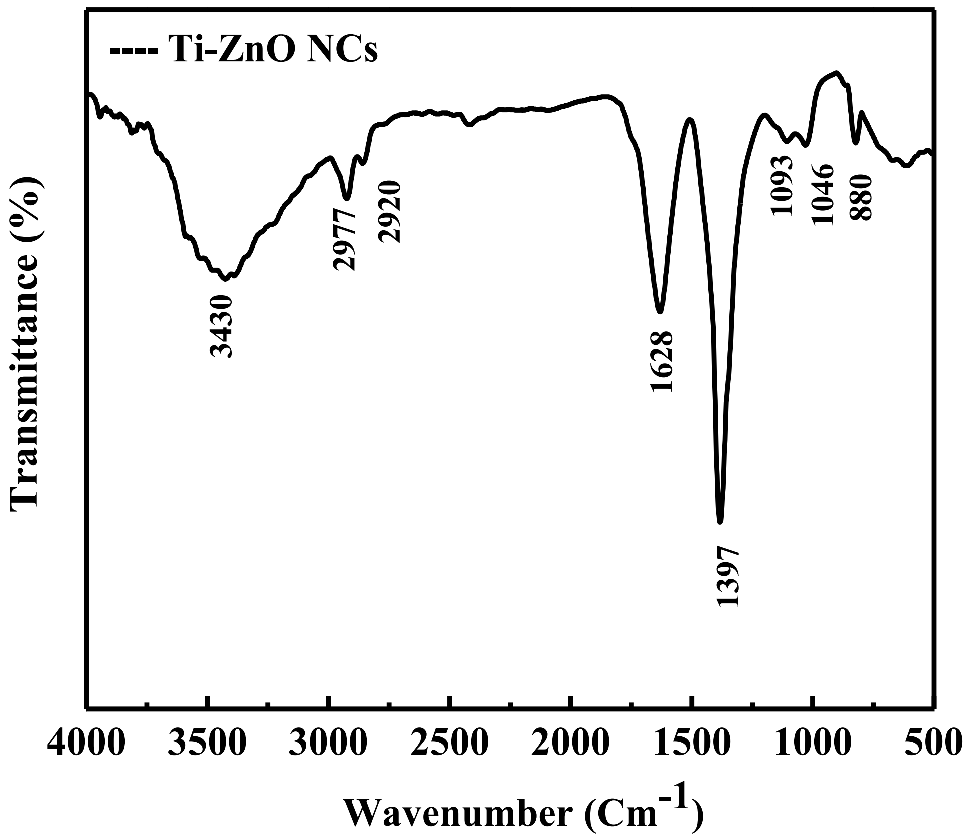

Fig. 2 FTIR spectrum of Ti-ZnO NCs

3.2.3 X-ray diffraction (XRD)

The XRD pattern of the synthesized Ti–ZnO NCs displayed well-defined diffraction peaks at 2θ values of 25.92°, 38.16°, 48.38°, 54.13°, 55.69°, 62.75°, 70.32°, and 75.55° in **Fig. 3**. The sharpness and intensity of these peaks confirm the crystalline nature of the prepared NCs. The peak at 25.92° can be attributed to the (101) plane of anatase TiO_2, while the peaks at 38.16°, 48.38°, and 55.69° correspond to the hexagonal phase

ZnO structure, matched with JCPDS Card No. 01-079-0208 for ZnO and 21-1272 for TiO_2. The coexistence of both Ti and ZnO diffraction peaks indicates the successful formation of a Ti–ZnO nanocomposite with a polycrystalline structure [45]. The crystallite size of the nanocomposite was calculated using the Debye–Scherrer formula:

$D = K\lambda / \beta \cos\theta$……..……..…..... (3)

The estimated average crystallite size was in the nanometre range, confirming the nanoscale nature of the material. The obtained crystalline structure is expected to enhance the photocatalytic and antimicrobial efficiency of the nanocomposite, as the intimate contact between TiO_2 and ZnO phases improves charge separation and suppresses electron–hoe recombination [46].

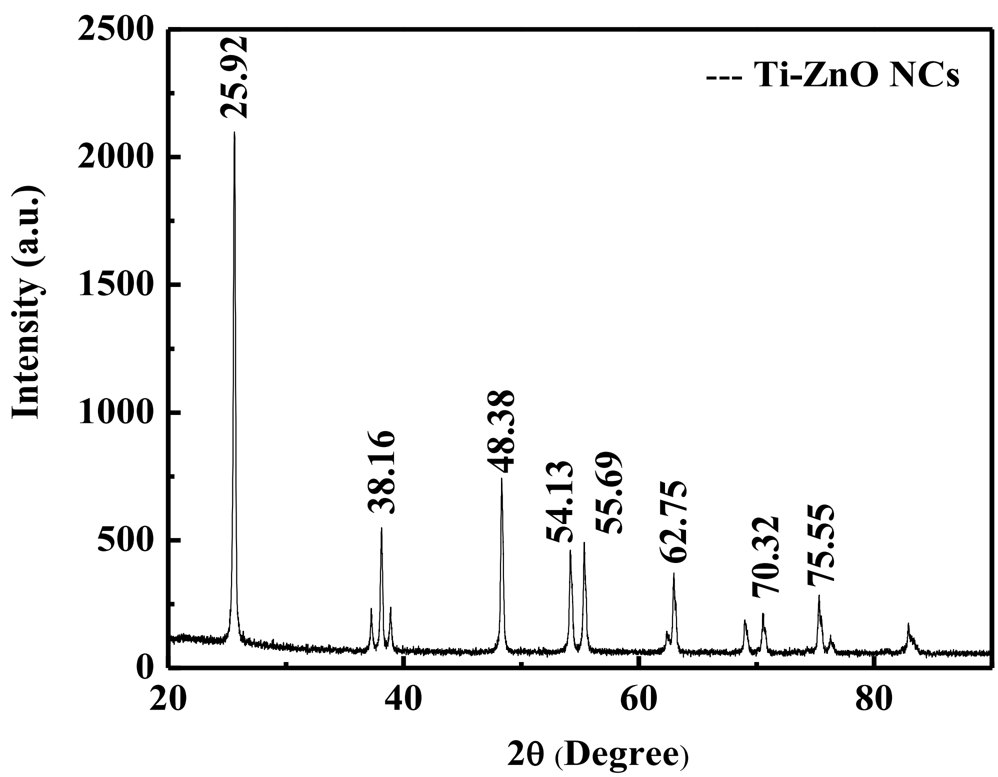

Fig. 3 XRD pattern of Ti-ZnO NCs

3.2.4 Scanning Electron Microscopy (SEM) and Energy Dispersive Spectroscopy (EDS)

The scanning electron microscopy (SEM) revealed that the Ti–ZnO NCs possess predominantly spherical morphology with an average particle size of approximately 33 nm. The nanoparticles were observed to be densely packed into grains, forming a smooth surface without detectable voids or cracks in **Fig. 4** [47]. Energy-dispersive X-ray spectroscopy (EDS) further confirmed the elemental composition, indicating the presence of titanium, zinc and oxygen as major constituents [48]. The EDS spectrum in **Fig.5** displayed a highly intense peak for titanium and comparatively weaker peaks for zinc and oxygen, with weight percentages of 59.25% Ti, 30.99% Zn, and 9.75% O, respectively shown in **Table 1**. The molecule of oxygen plays a crucial role in generating reactive oxygen species (ROS), which are directly linked to the antimicrobial efficacy and waste water treatment potential of Ti–ZnO NCs [49].

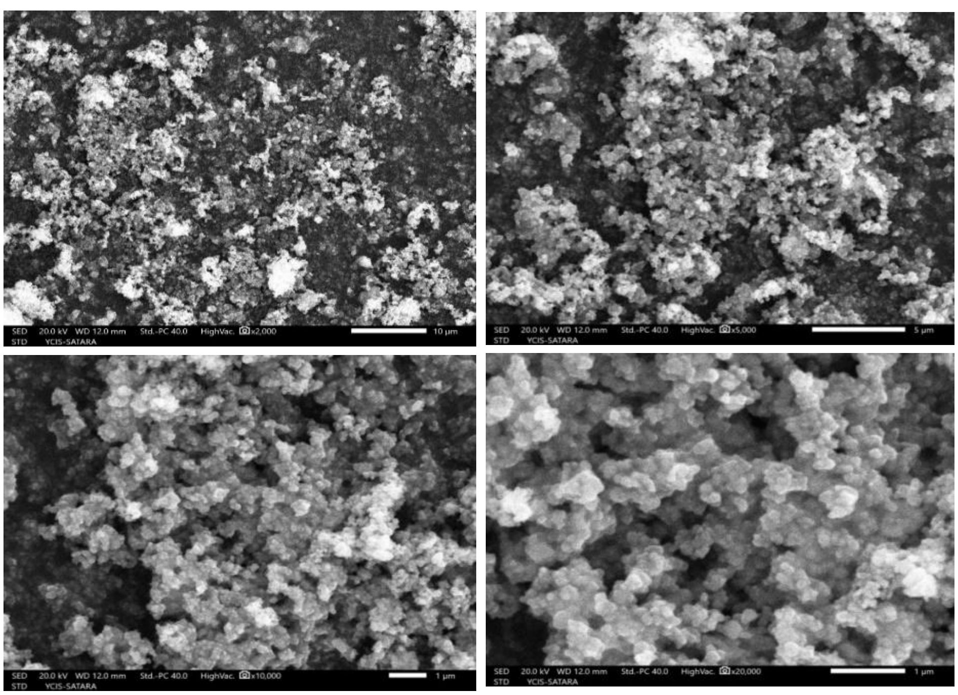

Fig. 4 Shown morphology of prepared Ti-ZnO NPs

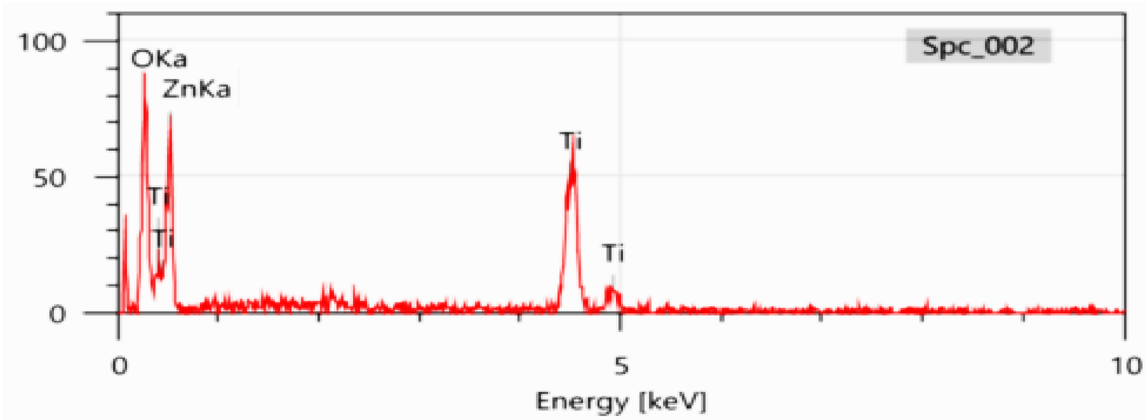

Fig. 5 EDS spectrum of Ti-ZnO NCs at 10.0 keV

Elements	**Line**	**Weight**	**Atomic %**
O	K	9.75	4.87
Ti	K	59.25	80.13
Zn	K	30.99	14.99
Total		**100.00**	**100.00**

Table 1: Element composition Ti-ZnO NCS by EDS analysis.

3.3 Antimicrobial Assay

Antimicrobial assays were performed to evaluate the antibacterial potential of Ti-ZnO nanocomposite (Ti-ZnO NCs). After 24 hours of incubation, the treated agar plates were examined to assess the formation of inhibition zones. The results, as presented in **Fig. 6** and **Table 2**. Notably, significant inhibitory effects were observed against *Staphylococcus aureus* NCIM-2654 (23.66 mm), *Bacillus cereus* NCIM-2703 (21.66 mm), *Proteus vulgaris* NCIM-2813 (16.66 mm), and *Salmonella* *typhi* NCIM-2501 (21.66 mm) as evidenced by the measurable zones of inhibition [50]. These findings suggest that the biosynthesized Ti-ZnO nanocomposites exhibit broad-spectrum antimicrobial properties, consistent with earlier studies highlighting the strong bactericidal and fungicidal performance of metal oxide nanoparticles due to their ability to generate reactive oxygen species and disrupt microbial cell membranes. The statistical graphical analysis of the antimicrobial study displayed in **Fig. 7.**

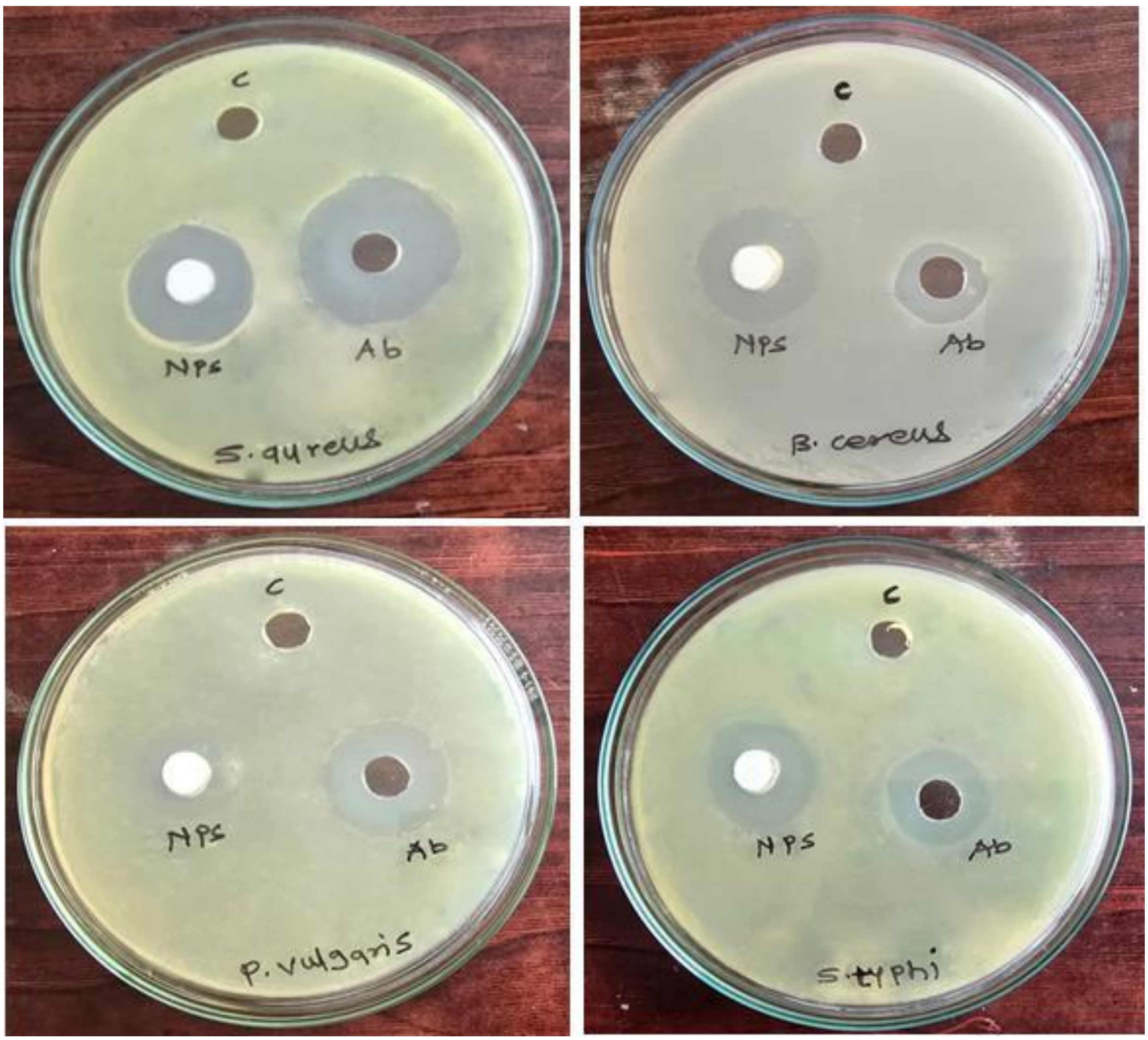

Entry	Antibacterial activity			
	Gram + Ve		Gram - Ve	
	Staphylococcus aureus (NCIM-2654)	*Bacillus cerus (NCIM - 2703)*	*Proteus vulgaris (NCIM - 2813)*	*Salmonella typhimurium (NCIM - 2501)*
Ti-ZnO NCs	**23.66 ± 0.57**	**21.66 ± 0.57**	**16.66 ± 0.57**	**21.66 ± 0.57**
Streptomycin Ab	**30.33 ± 0.57**	**16.33 ± 0.57**	**21.33 ± 0.57**	**20.66 ± 0.57**

Fig. 6 Antimicrobial activity on the *Staphylococcus aureus (NCIM -2654), Bacillus cereus (NCIM 2703), Proteus vulgaris (NCIM - 2813)* and *Salmonella typhimurium (NCIM-2501)* zone of inhibition for NPs-Nanoparticles, Ab-Antibiotic and C-Control.

Table. 2 Zone of inhibition due to Ti-ZnO NCs

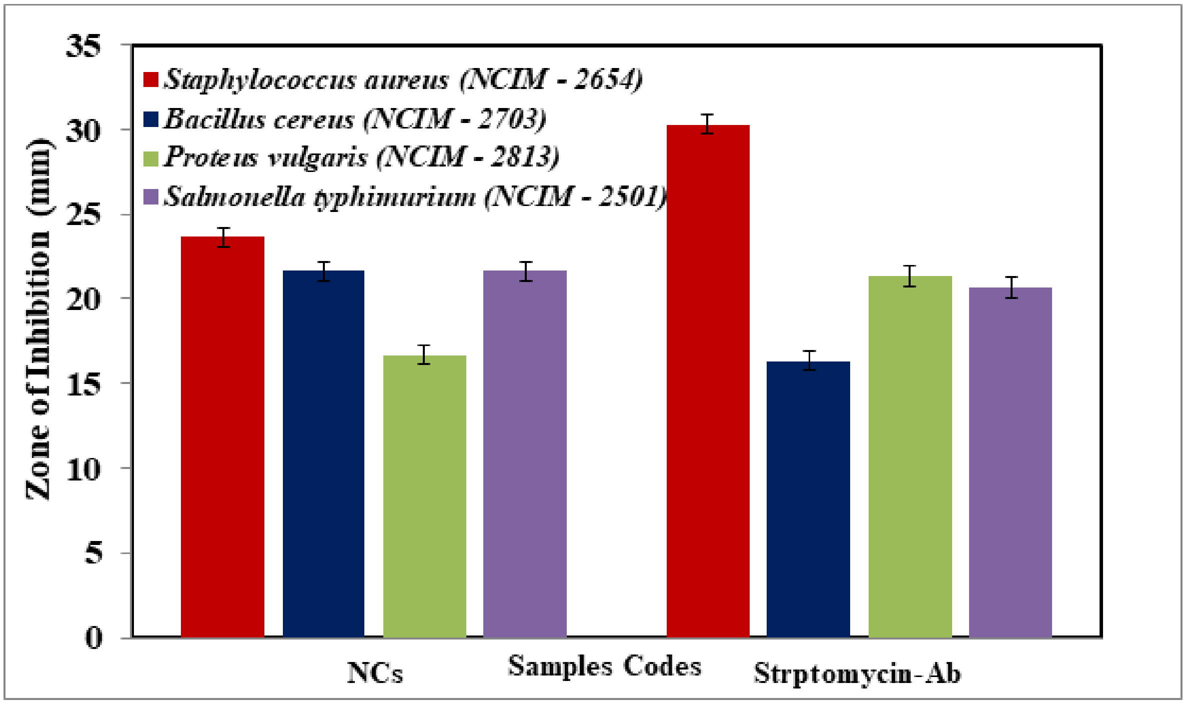

Fig. 7 The statistical analysis of NCs-Nanoparticles and Ab-Antibiotic against bacterial human pathogens

3.4 Anticancer activity

The cytotoxic potential of the Ti-ZnO nanocomposite was evaluated on MCF-7 breast cancer cells using the MTT assay, and the outcomes were compared with the standard . Anticancer drug 5-Fluorouracil (5-FU). The assay results are summarized in **Table 3** and represented in **Fig. 8**. At 20 µg/mL, the Ti-ZnO nanocomposite displayed 33.73% inhibition of MCF-7 cells, which is comparable to the standard drug (38.25%). With increasing concentrations, the inhibition rate of Ti-ZnO nanocomposite progressively improved, reaching 56.68% at 80 µg/mL and 54.38% at 100 µg/mL. In comparison, 5-FU exhibited 86.09% inhibition at 100 µg/mL, with an IC_{50} value of 39.33 µg/mL. The IC_{50} value of Ti–ZnO nanocomposite was 95.62 µg/mL, suggest that although the standard drug showed higher potency, the Ti-ZnO nanocomposite demonstrated significant anticancer activity, particularly at moderate to higher concentrations. Interestingly, the Ti-ZnO nanocomposite maintained substantial inhibition even at concentrations where 5-FU was more cytotoxic, indicating that the nanocomposite may provide controlled anticancer effect with potentially lower cytotoxicity to non-target cells [51].

Sr. No.	Sample Code	Concentration (µg/ml)	Absorbance at 510nm				% Inhibition	% of Viability	IC_{50} (µg/ml)
			Test 1	Test 2	Test 3	Mean			
1	**Control**	-	1.482	1.482	1.482	1.482	-		
2	**Standard (5, Flurour-acil)**	20	0.916	0.915	0.916	0.915	38.25%	61.75%	36.33
		40	0.732	0.729	0.734	0.731	50.67%	49.33%	
		60	0.507	0.504	0.502	0.504	65.99%	34.01%	
		80	0.315	0.312	0.314	0.313	78.87%	21.13%	
		100	0.208	0.205	0.207	0.206	86.09%	13.91%	
3	**Ti-ZnO NCs**	20	0.985	0.982	0.981	0.982	33.73%	66.26%	95.62
		40	0.812	0.810	0.811	0.811	45.27%	54.73%	
		60	0.778	0.776	0.781	0.778	47.50%	52.50%	
		80	0.645	0.640	0.641	0.642	56.68%	43.32%	
		100	0.678	0.674	0.676	0.676	54.38%	45.61%	

Table 3: Effects of NCS and standard drug against MCF-7 Cell lines

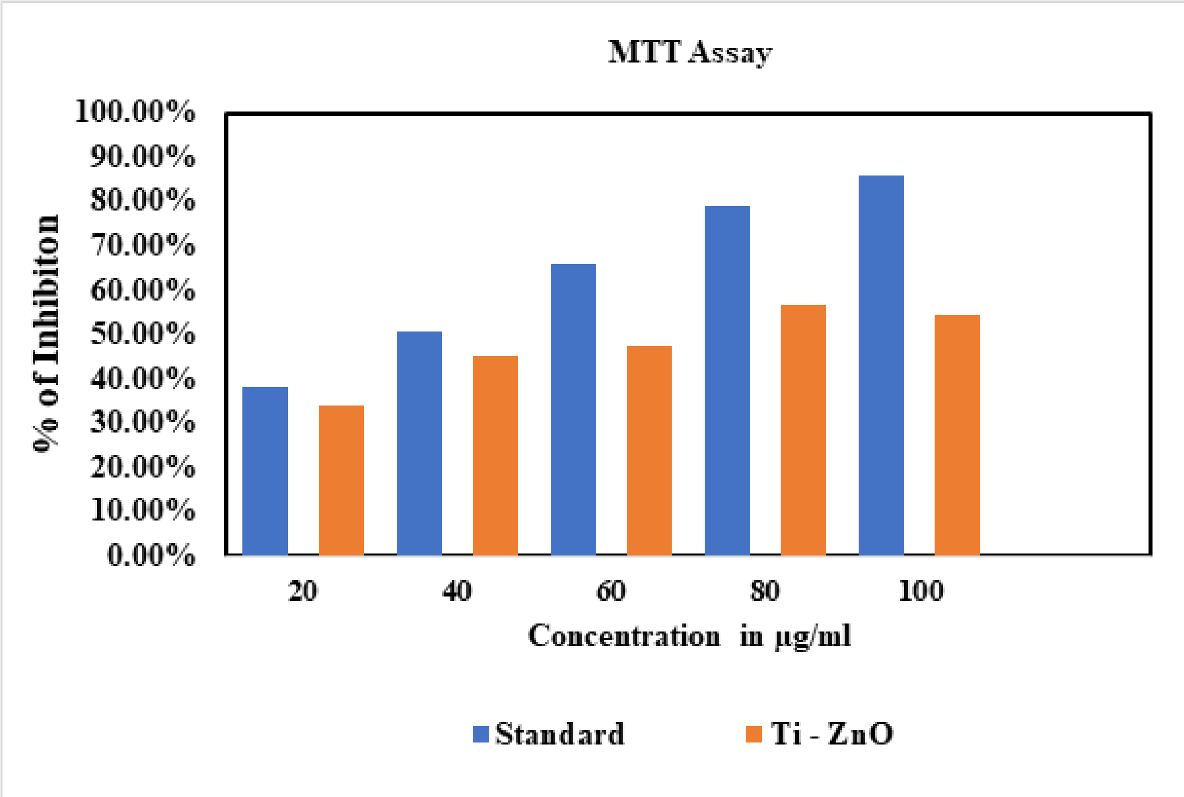

Fig. 8 Graphical representation of percent of inhibition (IC_{50}) against MCF7 Cell lines by standard drug and Ti-ZnO NCs.

3.5 Antioxidant Activity

The DPPH (2,2-diphenyl-1-picrylhydrazyl) radical scavenging assay is widely used to measure antioxidant activity. A decrease in absorbance at 517 nm (or 540 nm depending on setup) indicates the ability of a compound to donate hydrogen atoms or electrons, neutralizing free radicals both ascorbic acid and TiO_2–ZnO showed dose-dependent antioxidant activity shown in **Fig. 9** and **Table 4**. At lower concentrations (20-40µg/ml), ascorbic acid had higher inhibition. At higher concentrations (80–100 µg/ml), TiO_2–ZnO nearly matched the scavenging activity of ascorbic acid. The comparable inhibition pattern highlights the potential of TiO_2–ZnO as a promising antioxidant nanomaterial. The strong antioxidant activity of TiO_2–ZnO can be attributed to high surface-to-volume ratio of nanoparticles, enhancing free radical interaction. Synergistic effect of Ti with Zn oxides, which improves electron transfer properties. Such antioxidant nanomaterials are gaining interest for biomedical applications, including anti-aging, anti-inflammatory and protective roles against oxidative stress [52].

Sr. No.	Sample Code	Concentration (µg/ml)	Absorbance at 510nm				% Inhibition	IC_{50} (µg/ml)
			Test 1	Test 2	Test 3	Mean		
1	**Control**	-	1.92	1.92	1.92	1.92	-	
2	**Standard (Ascorbic Acid)**	20	1.08	1.05	1.06	1.06	45%	39.02
		40	0.91	0.93	0.90	0.91	52.84%	
		60	0.78	0.77	0.77	0.77	60.10%	
		80	0.60	0.61	0.59	0.60	68.91%	
		100	0.49	0.47	0.45	0.47	75.64%	
3	**Ti-ZnO**	20	1.21	1.20	1.18	1.19	38.34%	55.10
		40	1.02	1.01	1.02	1.01	47.66%	
		60	0.88	0.85	0.87	0.86	55.44%	
		80	0.63	0.64	0.62	0.63	67.35%	
		100	0.54	0.51	0.53	0.52	73.05%	

Table. 4 Radical scavenging activity Ti-ZnO NCs and Ascorbic Acid

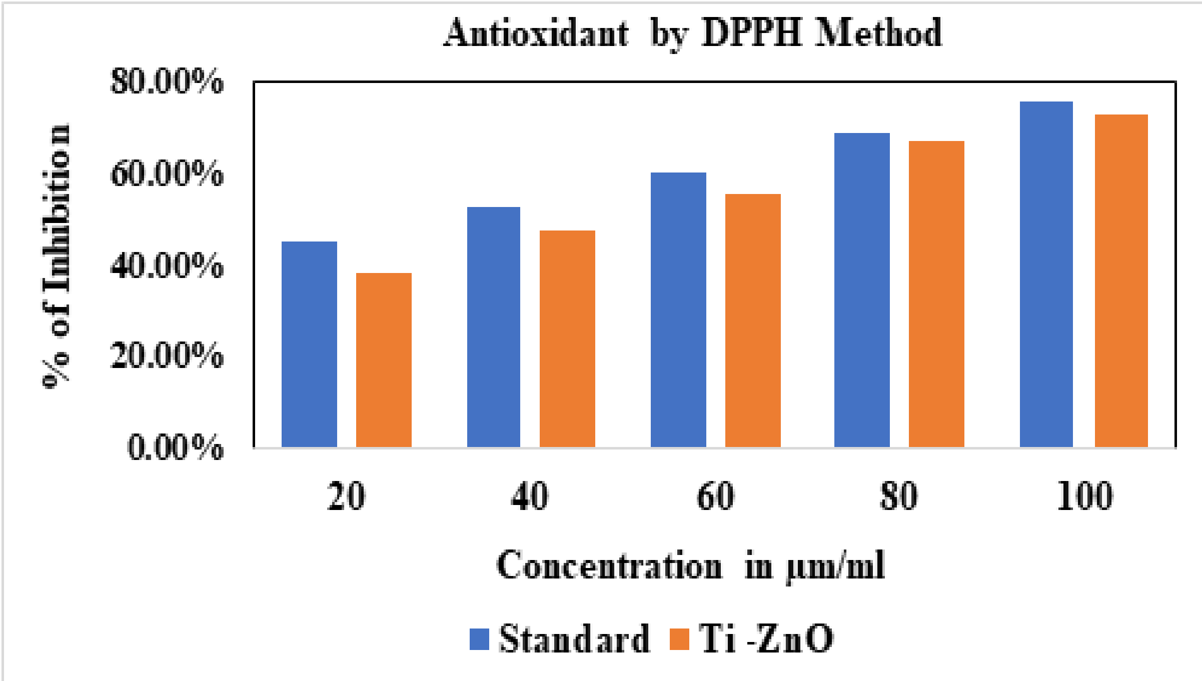

Fig. 9 Ti-ZnO NCs-DPPH free radical scavenging activity

3.6 Antidiabetic Activity

Ti–ZnO nanocomposites exhibited a concentration-dependent increase in enzyme inhibition, indicating effective suppression of α-amylase activity displayed in **Table 5**. Although the standard drug acarbose showed higher inhibitory activity with an IC_{50} value of 39.02 µg/ml, Ti–ZnO nanocomposites demonstrated notable inhibition with an IC_{50} value of 55.10 µg/ml. The comparative inhibitory trend between the standard and Ti–ZnO nanocomposites across different concentrations is clearly illustrated in the bar graph **Fig.10** confirming their potential antidiabetic activity [53].

			α amylase enzyme inhibition assay					
Sr. No.	**Sample Code**	**Concentration (µg/ml)**	**Absorbance at 540 nm**				**% of Inhibition**	**IC_{50} (µg/ml)**
			Test 1	**Test 2**	**Test 3**	**Mean**		
1	**Control**		1.53	1.53	1.53	1.53		
2	**Standard (Acarbose)**	20	0.81	0.83	0.81	0.81	47.05%	
		40	0.74	0.77	0.75	0.75	50.98%	
		60	0.60	0.58	0.60	0.59	61.43%	39.02
		80	0.41	0.41	0.40	0.40	73.85%	
		100	0.30	0.27	0.28	0.28	81.69%	
3	**Ti-ZnO NCs**	20	0.96	0.92	0.94	0.94	38.56%	
		40	0.81	0.80	0.80	0.80	47.71%	
		60	0.70	0.68	0.71	0.69	54.90%	55.10
		80	0.59	0.55	0.57	0.57	62.74%	
		100	0.38	0.35	0.37	0.36	76.47%	

Table. 5 Anti-diabetic assay by alpha amylase method.

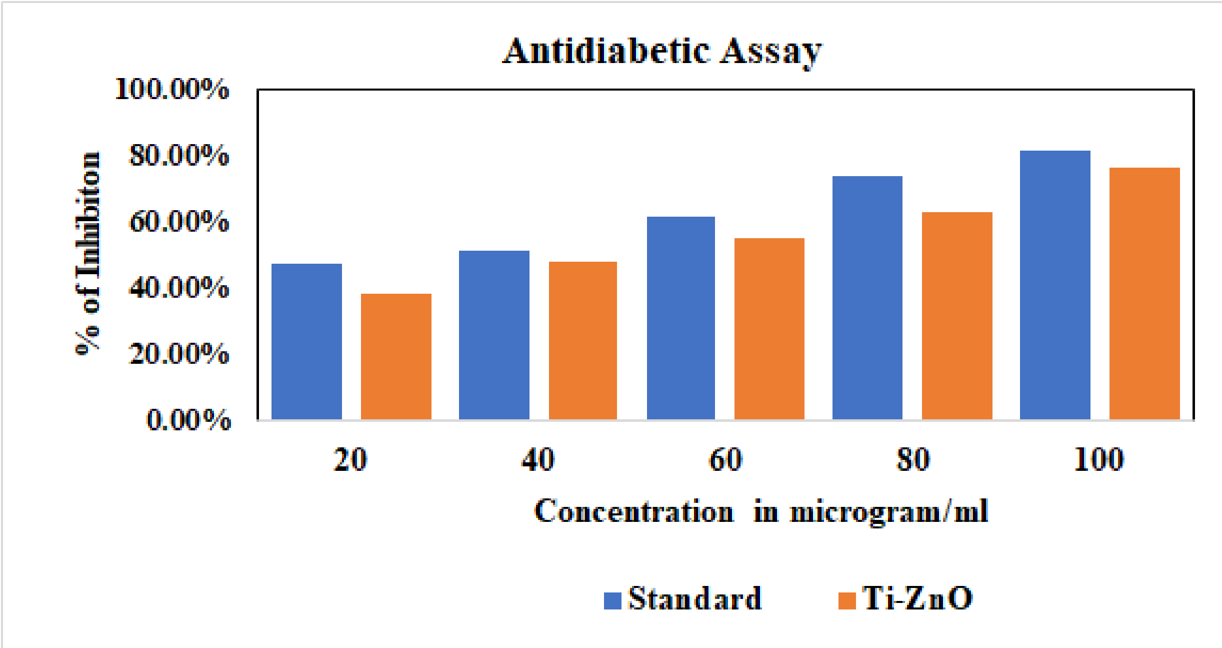

Fig. 10 Graphical representation of Anti-diabetic assay by alpha amylase method

4. Conclusion

The present study demonstrates the successful microbial synthesis of Ti–ZnO nanocomposites using *Aspergillus niger* a fungal-mediated approach. This is an eco-friendly and sustainable alternative to conventional chemical methods that often involve toxic reagents. Comprehensive physicochemical characterization confirmed the formation of a stable nanocomposite structure. UV–Visible spectroscopy indicated a characteristic absorption peak at 272 nm, while XRD analysis verified the coexistence of anatase TiO_2 and hexagonal ZnO phases with nanoscale nano composite crystallinity. SEM observations revealed aggregated, densely packed nanoparticles with an average size of approximately 33 nm, and EDS analysis confirmed the presence of Ti, Zn, and O elements, validating the successful pure formation of the Ti–ZnO nanocomposite. Importantly, the synthesized nanocomposites exhibited remarkable multifunctional biological activities. They demonstrated broad-spectrum antimicrobial activity against both Gram-positive and Gram-negative bacterial strains, indicating strong antibacterial potential. Furthermore, the nanocomposites showed significant dose-dependent cytotoxic effects against MCF-7 breast cancer cells, suggesting their potential role in anticancer applications. In addition, notable antioxidant activity in the DPPH assay and effective α-amylase inhibition highlighted their promising antidiabetic potential. Overall, the findings emphasize that fungal-mediated Ti–ZnO nanocomposites represent a promising multifunctional nanomaterial with significant potential for biomedical and therapeutic applications. The eco-friendly synthesis strategy, combined with enhanced biological activities, makes these nanocomposites attractive candidates for future development in nanomedicine, drug delivery and antimicrobial formulations. Further in vivo investigations and mechanistic studies are recommended to fully explore their clinical and environmental applicability.

5. Reference

1. Roco, Mihail C. "Nanotechnology: convergence with modern biology and medicine." *Current opinion in biotechnology* 14, no. 3 (2003): 337-346.
2. Whitesides, George M. "The'right'size in nanobiotechnology." *Nature biotechnology* 21, no. 10 (2003): 1161-1165.
3. Salata, Oleg V. "Applications of nanoparticles in biology and medicine." *Journal of nanobiotechnology* 2, no. 1 (2004): 3.
4. Moghimi, S. Moein, A. Christy Hunter, and J. Clifford Murray. "Nanomedicine: current status and future prospects." *The FASEB journal* 19, no. 3 (2005): 311-330.
5. Jain, Kewal K. "Nanomedicine: application of nanobiotechnology in medical practice." *Medical Principles and Practice* 17, no. 2 (2008): 89-101.

6. Ahmed, Shakeel, and Saiqa Ikram. "Silver nanoparticles: one pot green synthesis using Terminalia arjuna extract for biological application." *J. Nanomed. Nanotechnol* 6, no. 4 (2015): 1-6.

7. Durán, Nelson, Priscyla D. Marcato, Marcela Durán, Alka Yadav, Aniket Gade, and Mahendra Rai. "Mechanistic aspects in the biogenic synthesis of extracellular metal nanoparticles by peptides, bacteria, fungi, and plants." *Applied microbiology and biotechnology* 90, no. 5 (2011): 1609-1624.

8. Kołodziejczak-Radzimska, Agnieszka, and Teofil Jesionowski. "Zinc oxide—from synthesis to application: a review." *Materials* 7, no. 4 (2014): 2833-2881.

9. Ozgur, U., Ya I. Alivov, C. Liu, A. Teke, M. A. Reshchikov, S. Dogan, and V. Avrutin. "Cho SJ and Morkoc H." *J. Appl. Phys.* 2005 (2005): 98.

10. Wang, Zhong Lin. "Zinc oxide nanostructures: growth, properties and applications." *Journal of physics: condensed matter* 16, no. 25 (2004): R829-R858.

11. Iravani, Siavash. "Green synthesis of metal nanoparticles using plants." *Green chemistry* 13, no. 10 (2011): 2638-2650.

12. Singh, Om V., ed. *Bio-nanoparticles: biosynthesis and sustainable biotechnological implications*. John Wiley & Sons, 2015.

13. Sharma, Rhydum, and Ashutosh Tripathi. "Green synthesis of nanoparticles and its key applications in various sectors." *Materials Today: Proceedings* 48 (2022): 1626-1632.

14. Sharma, Rhydum, and Ashutosh Tripathi. "Green synthesis of nanoparticles and its key applications in various sectors." *Materials Today: Proceedings* 48 (2022): 1626-1632.

15. Mittal, Stuti, and Arpita Roy. "Fungus and plant-mediated synthesis of metallic nanoparticles and their application in degradation of dyes." In *Photocatalytic degradation of dyes*, pp. 287-308. Elsevier, 2021.

16. Prasad, Ram. *Microbial nanobionics*. Springer International Publishing, 2019.

17. Thakkar, Kaushik N., Snehit S. Mhatre, and Rasesh Y. Parikh. "Biological synthesis of metallic nanoparticles." *Nanomedicine: nanotechnology, biology and medicine* 6, no. 2 (2010): 257-262.

18. Rangaswamy, V. "Synthesis and Applications of Fungal-Mediated Nanoparticles." *Microbial Processes for Synthesizing Nanomaterials* (2023): 113.
19. Siddiqi, Khwaja Salahuddin, Aziz Ur Rahman, N. Tajuddin, and Azamal Husen. "Properties of zinc oxide nanoparticles and their activity against microbes." *Nanoscale research letters* 13, no. 1 (2018): 141.
20. Rack, H. J., and J. I. Qazi. "Titanium alloys for biomedical applications." *Materials Science and Engineering: C* 26, no. 8 (2006): 1269-1277.
21. Elias, Carlos Nelson, Marc André Meyers, Ruslan Z. Valiev, and Sérgio Neves Monteiro. "Ultrafine grained titanium for biomedical applications: An overview of performance." *Journal of Materials Research and Technology* 2, no. 4 (2013): 340-350.
22. Ozawa, Kenichi, Susumu Yamamoto, Kazuhiko Mase, and Iwao Matsuda. "A surface science approach to unveiling the TiO2 photocatalytic mechanism: Correlation between photocatalytic activity and carrier lifetime." *e-Journal of Surface Science and Nanotechnology* 17 (2019): 130-147.
23. Diebold, Ulrike. "The surface science of titanium dioxide." *Surface science reports* 48, no. 5-8 (2003): 53-229.
24. Hoffmann, Michael R., Scot T. Martin, Wonyong Choi, and Detlef W. Bahnemann. "Environmental applications of semiconductor photocatalysis." *Chemical reviews* 95, no. 1 (1995): 69-96.
25. Gold, Karli, Buford Slay, Mark Knackstedt, and Akhilesh K. Gaharwar. "Antimicrobial activity of metal and metal-oxide based nanoparticles." *Advanced Therapeutics* 1, no. 3 (2018): 1700033.
26. Survase, Avinash Ashok, and Shivangi Shivraj Kanase. "Green synthesis of TiO2 nanospheres from isolated Aspergillus eucalypticola SLF1 and its multifunctionality in nanobioremediation of CI Reactive Blue 194 with antimicrobial and antioxidant activity." *Ceramics International* 49, no. 10 (2023): 14964-14980.
27. Bhoomanee, Chawalit, Pipat Ruankhama, Supab Choopun, Aschariya Prathan, and Duangmanee Wongratanaphisan. "Effect of al-doped ZnO for electron transporting layer in planar perovskite solar cells." *Materials*

Today: Proceedings 17 (2019): 1259-1267.

28. Mouhamad, Raghad S., Khlood Abedalelah Al Khafaji, Mohammad Hussein Al-Dharob, and Entisar E. Al-Abodi. "Antifungal, antibacterial and anti-yeast activities evaluation of oxides of silver, zinc and titanium nanoparticles." *Chem Int* 8, no. 4 (2022): 159-166.
29. Mosmann, Tim. "Rapid colorimetric assay for cellular growth and survival: application to proliferation and cytotoxicity assays." *Journal of immunological methods* 65, no. 1-2 (1983): 55-63.
30. Sánchez-Moreno, Concepción, Jose A. Larrauri, and Fulgencio Saura-Calixto. "A procedure to measure the antiradical efficiency of polyphenols." *Journal of the Science of Food and Agriculture* 76, no. 2 (1998): 270-276.
31. Zephy, Doddigarla, and Jamal Ahmad. "Type 2 diabetes mellitus: role of melatonin and oxidative stress." *Diabetes & metabolic syndrome: clinical research & reviews* 9, no. 2 (2015): 127-131.
32. Maru, Apexa, C. M. Panchasara, K. N. Rathod, Hetal Boricha, Khushal Sagapariya, Bhagyashree Udeshi, Ajay Vaishnani et al. "UV–Visible spectroscopy and dielectric studies of ZnO/TiO2 composite." *Bulletin of Materials Science* 46, no. 3 (2023): 150.
33. Gunasekaran, Anguraj, Ashok Kumar Rajamani, Chandrasekar Masilamani, Inmozhi Chinnappan, Uthrakumar Ramamoorthy, and Kasinathan Kaviyarasu. "Synthesis and characterization of ZnO doped TiO2 nanocomposites for their potential photocatalytic and antimicrobial applications." *Catalysts* 13, no. 2 (2023): 215.
34. Cullity, B. D., and S. R. Stock. "Elements of X-ray Diffraction, Prentice Hall Inc." *New York* (2001).
35. Hajipour, Mohammad J., Katharina M. Fromm, Ali Akbar Ashkarran, Dorleta Jimenez De Aberasturi, Idoia Ruiz De Larramendi, Teofilo Rojo, Vahid Serpooshan, Wolfgang J. Parak, and Morteza Mahmoudi. "Antibacterial properties of nanoparticles." *Trends in biotechnology* 30, no. 10 (2012): 499-511.
36. Hansen, Morten Bagge, Svend Erik Nielsen, and Kurt Berg. "Re-examination and further development of a precise and rapid dye method for measuring cell growth/cell

kill." *Journal of immunological methods* 119, no. 2 (1989): 203-210.

37. Baliyan, Siddartha, Riya Mukherjee, Anjali Priyadarshini, Arpana Vibhuti, Archana Gupta, Ramendra Pati Pandey, and Chung-Ming Chang. "Determination of antioxidants by DPPH radical scavenging activity and quantitative phytochemical analysis of Ficus religiosa." *Molecules* 27, no. 4 (2022): 1326.
38. El-Borady, Ola M., and Ahmed F. El-Sayed. "Synthesis, morphological, spectral and thermal studies for folic acid conjugated ZnO nanoparticles: potency for multi-functional bio-nanocomposite as antimicrobial, antioxidant and photocatalytic agent." *Journal of Materials Research and Technology* 9, no. 2 (2020): 1905-1917.
39. Gharpure, Saee, Aman Akash, and Balaprasad Ankamwar. "A review on antimicrobial properties of metal nanoparticles." *Journal of nanoscience and nanotechnology* 20, no. 6 (2020): 3303-3339.
40. Sánchez-Moreno, Concepción, Jose A. Larrauri, and Fulgencio Saura-Calixto. "A procedure to measure the antiradical efficiency of polyphenols." *Journal of the Science of Food and Agriculture* 76, no. 2 (1998): 270-276.
41. Zephy, Doddigarla, and Jamal Ahmad. "Type 2 diabetes mellitus: role of melatonin and oxidative stress." *Diabetes & metabolic syndrome: clinical research & reviews* 9, no. 2 (2015): 127-131.
42. Maru, Apexa, C. M. Panchasara, K. N. Rathod, Hetal Boricha, Khushal Sagapariya, Bhagyashree Udeshi, Ajay Vaishnani et al. "UV–Visible spectroscopy and dielectric studies of ZnO/TiO2 composite." *Bulletin of Materials Science* 46, no. 3 (2023): 150.
43. Kurniawan, Yehezkiel Steven, and Leny Yuliati. "Activity enhancement of p25 titanium dioxide by zinc oxide for photocatalytic phenol degradation." *Bulletin of Chemical Reaction Engineering & Catalysis* 16, no. 2 (2021): 310-319.
44. Gunasekaran, Anguraj, Ashok Kumar Rajamani, Chandrasekar Masilamani, Inmozhi Chinnappan, Uthrakumar Ramamoorthy, and Kasinathan Kaviyarasu. "Synthesis and characterization of ZnO doped TiO2 nanocomposites for their potential photocatalytic and antimicrobial

applications." *Catalysts* 13, no. 2 (2023): 215.

45. Jiang, Jinhuan, Jiang Pi, and Jiye Cai. "The advancing of zinc oxide nanoparticles for biomedical applications." *Bioinorganic chemistry and applications* 2018, no. 1 (2018): 1062562.
46. Zhang, Huanjun, Guohua Chen, and Detlef W. Bahnemann. "Photoelectrocatalytic materials for environmental applications." *Journal of Materials Chemistry* 19, no. 29 (2009): 5089-5121.
47. Li, Qilin, Shaily Mahendra, Delina Y. Lyon, Lena Brunet, Michael V. Liga, Dong Li, and Pedro JJ Alvarez. "Antimicrobial nanomaterials for water disinfection and microbial control: potential applications and implications." *Water research* 42, no. 18 (2008): 4591-4602.
48. Sangiorgi, Nicola, Lucrezia Aversa, Roberta Tatti, Roberto Verucchi, and Alessandra Sanson. "Spectrophotometric method for optical band gap and electronic transitions determination of semiconductor materials." *Optical Materials* 64 (2017): 18-25.
49. Usman, Muhammad Sani, Mohamed Ezzat El Zowalaty, Kamyar Shameli, Norhazlin Zainuddin, Mohamed Salama, and Nor Azowa Ibrahim. "Synthesis, characterization, and antimicrobial properties of copper nanoparticles." *International journal of nanomedicine* (2013): 4467-4479.
50. Hajipour, Mohammad J., Katharina M. Fromm, Ali Akbar Ashkarran, Dorleta Jimenez De Aberasturi, Idoia Ruiz De Larramendi, Teofilo Rojo, Vahid Serpooshan, Wolfgang J. Parak, and Morteza Mahmoudi. "Antibacterial properties of nanoparticles." *Trends in biotechnology* 30, no. 10 (2012): 499-511.
51. Baliyan, Siddartha, Riya Mukherjee, Anjali Priyadarshini, Arpana Vibhuti, Archana Gupta, Ramendra Pati Pandey, and Chung-Ming Chang. "Determination of antioxidants by DPPH radical scavenging activity and quantitative phytochemical analysis of Ficus religiosa." *Molecules* 27, no. 4 (2022): 1326.
52. El-Borady, Ola M., and Ahmed F. El-Sayed. "Synthesis, morphological, spectral and thermal studies for folic acid conjugated ZnO nanoparticles: potency for multi-functional bio-

nanocomposite as antimicrobial, antioxidant and photocatalytic agent." *Journal of Materials Research and Technology* 9, no. 2 (2020): 1905-1917.

53. Shafique, Shizza, Zubaah Khalid, Saira Arif, Zobia Noreen, Lubna Tabassam, and Muhammad Waseem. "ZnO, TiO_2 and Ag_2O decorated MWCNTs for enhanced antibacterial and antidiabetic activities." *Inorganic Chemistry Communications* 163 (2024): 112383.